Inorganic Chemistry

ARTICLE

pubs.acs.org/IC

Polytypism in the Lithium−Aluminum Layered Double Hydroxides: The $[LiAl_2(OH)_6]^+$ Layer as a Structural Synthon

Sylvia Britto and P. Vishnu Kamath*

Department of Chemistry, Central College, Bangalore University, Bangalore 560 001, India

Supporting Information

ABSTRACT: The $[LiAl_2(OH)_6]^+$ layer obtained from gibbsite−$Al(OH)_3$ belongs to the layer group symmetry *P*-312/*m*. This layer satisfies the defining characteristics of a synthon in that it predicts all the polymorphic modifications of the layered double hydroxides of Li and Al. The various possible ways of stacking these layers can be derived by the systematic elimination of the principal symmetry elements comprising the layer group. This approach yields the complete universe of possible structures. When the 3 axis of the layer is conserved in the stacking, the resultant crystal adopts the structure of the 1H, 2H, or 3R polytypes (H, hexagonal; R, rhombohedral). When the 3 axis is destroyed and the 2/*m* axis is retained, the crystal adopts monoclinic symmetry and crystallizes in the structures of the $1M_1$ or $1M_2$ (M, monoclinic) polytypes; the two polytypes differ only in their translational component. Experimentally, gibbsite-based precursors yield the 2H polytype, and bayerite-based precursors yield the 1M polytype. Faulted structures incorporating differently oriented $1M_1$ motifs or a mixture of $1M_1$ and $1M_2$ motifs are also obtained. These stacking faults result in cation disorder along the *c* axis and produce signature effects on the line shapes of select reflections in the powder X-ray diffraction patterns. This symmetry-guided approach is general and can be extended to other classes of layered solids.

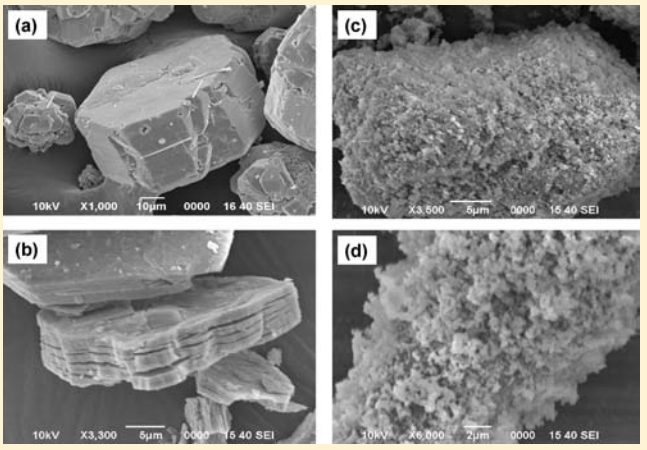

INTRODUCTION

A sound understanding of crystal chemistry (either organic or inorganic) requires recognition of interrelationships between different crystal structures. In supramolecular chemistry, this is achieved by the recognition of a specific structural unit within the crystal (also a supermolecule) which repeats itself across diverse systems. Such a structural unit is called a supramolecular synthon.[1,2] Corey[3] originally defined a synthon as 'a structural unit within a molecule which can be formed or assembled by known or conceivable synthetic operations'. It had been defined by Corey as primarily an entity that aids in synthesis. Given the fact that design in chemical synthesis is now considered to be conceptually impossible,[4] the supramolecular synthon introduced by Desiraju, despite being defined in a sense similar to the synthon, is more an entity that enables a simplification of the understanding of crystal structures than something that aids in synthesis.

Although claimed to be generally applicable to all solids, the idea of a supramolecular synthon has been applied to only organic molecular solids and its successful use is predicated upon (i) recognition of a molecule as a repeating unit, (ii) recognition of the intermolecular connectivities, and (iii) identification of patterns of interactions that repeat across many different systems. Where no discrete recognizable molecular unit exists, as in inorganic solids with extended ionocovalent bonding, the approach needs to be rearticulated in different terms.

The recognition of simple structural units is not unique to organic solid state chemistry. The design and synthesis of inorganic solids from 2D building blocks was described earlier by Cario and co-workers,[5,6] who recognized that certain building units such as those derived from the fluorite, rock salt, or perovskite structures appear across a range of structures and may be combined to give rise to new inorganic solids. Two criteria were recognized as being essential to realize a successful stacking of two different layers: (i) structural, in the manner of a good match of the in-plane lattice dimensions of the two layers, and (ii) electronic, to secure charge neutrality. This approach, while yielding new structures, does not explore the universe of possible stacking sequences.

A more general approach to predict a cohort of (meta)stable structures is to compute the energy of all possible configurations for any given composition, an approach known as the 'energy landscape' method.[7,8] In a modification of this approach, the energies of all possible configurations of specific building units, rather than atoms, are computed to arrive at the possible

Received: February 15, 2011
Published: May 23, 2011

structures.[9,10] All these approaches are successful to varying degrees for small- to moderate-sized unit cells. However, these techniques are computationally very expensive and therefore unfeasible for systems with large unit cells. In such cases, a much simpler building block approach that relies upon geometric and symmetry restrictions would have to be invoked.

Many authors have employed secondary building units (SBU) in a qualitative, noncomputational approach to understand the crystal structures of metal organic framework solids (MOFs).[11,12] In their perception, the SBU is only a topological entity defined by covalently bonded connectivities and one that does not take into account the wide range of weak interactions, which are now universally accepted as being important structure-directing interactions.

This paper is an attempt to evolve a '(supramolecular) synthon-like' approach toward the understanding and prediction of structures of condensed (as opposed to framework) solids with extended bonding. As an illustration of our approach, we wish to begin with layered materials for the following reasons:

(1) In an extended layered solid there is no recognizable molecular unit. In as much as such a solid departs in character from the molecular solid, any success in the application of the synthon approach to such solids will mark a conceptual advance in supramolecular chemistry.
(2) Many weak interactions manifest themselves in layered solids, with the possibility of a diversity of interlayer connectivities, and thereby layered solids are more suited for the extension of the synthon approach compared to others where the bonding is exclusively covalent or strongly ionic.

In an earlier paper devoted to the study of interpolytype transformations in layered hydroxides,[13] we defined a 'structural synthon' as a certain packing of atoms that extends infinitely in two dimensions. The $[MX_2]$ layer comprising edge-sharing $[MX_6]$ octahedra (M = metal ion, X = anion) seen in a wide range of solids was put forth as an example of such a 'structural synthon'.

One of the weaknesses of the supramolecular synthon approach to the understanding of crystal structures is that there is no rigorous logically derivable relationship between the molecular symmetry, the local symmetry of the synthon, and the eventual crystal symmetry. There is at best a general understanding that centrosymmetric structures are preferred.[1]

Within the structural synthon approach however symmetry criteria guided by the symmetry of the synthon itself determines the different possible three-dimensional structural arrangements that may be arrived at from one particular synthon. For instance, the $[MX_2]$ layers may be stacked one above the other in a number of ways to yield a diversity of polytypes with the possible stacking modes being guided by the symmetry of the $[MX_2]$ layer.

Although a clear one to one analogy between the supramolecular synthon and the structural synthon is not possible due to the numerous conceptual differences between molecules/supermolecules (organic crystals) and inorganic solids, the structural synthon has in common with the supramolecular synthon the following defining features:

it helps in structure prediction (by predicting the realizable polytypes),
it simplifies the understanding of crystal structures of diverse systems,
it determines the nature of interlayer interactions, and
it repeats itself across diverse materials.

To further characterize the features of a structural synthon, we focus upon one particular class of materials—the layered double hydroxides (LDHs).[14] We do so as these materials provide two structural synthons: one derived from brucite, $Mg(OH)_2$, and the other from gibbsite/bayerite, $Al(OH)_3$.[15]

The brucite-based LDHs (also known as II−III LDHs) are built up of layers of the $[MX_2]$ type, having the composition $[M_x^{II}M'_{1-x}{}^{III}(OH)_2]^{x+}$. The positive charge is compensated by the intercalation of anions such as Cl^-, Br^-, CO_3^{2-}, and SO_4^{2-} in the interlayer region to yield solids having the composition $[M_x^{II}M'_{1-x}{}^{III}(OH)_2][A^{n-}]_{x/n}\cdot mH_2O$.[14] The polytype diversity of these materials, both expected and observed,[16,17] has been extensively explored, and it is often the coordination preference of the interlayer ion that directs the stacking.[18]

LDHs may also be derived from $Al(OH)_3$. The $[Al(OH)_3]$ layer is also similar to the $[MX_2]$ layer, except that one-third of the cation sites are vacant. The layer composition is given as $[Al_{2/3}\square_{1/3}(OH)_2]$. The vacancies are ordered, yielding an a parameter of ~5.1 Å compared to a = 3.1 Å for the $[MX_2]$ layer. The vacancies in the layer may be stuffed with Li^+ to yield cation-ordered positively charged layers having the composition $[Li_{1/3}Al_{2/3}(OH)_2]^{1/3+}$. For brevity, we refer to this layer as the Li−Al layer. Intercalation of anions and water molecules in the interlayer region results in solids having the composition $[Li_{1/3}Al_{2/3}(OH)_2][A^{n-}]_{1/3n}\cdot xH_2O$.[19] The Li−Al LDHs could be derived from either gibbsite[20] or bayerite,[21] and the two classes of LDHs have very different structures. For instance, the Li−Al−Cl LDH obtained from gibbsite crystallizes in hexagonal symmetry,[22] while that obtained from bayerite crystallizes in monoclinic symmetry.[23] In addition, each class can potentially exhibit further polytypism,[24] thereby increasing the diversity of possible structures. This paper is an attempt to evolve a unified approach to the understanding of these structures and gain insights into their inter-relationships.

Many studies have been reported of Li−Al LDHs containing intercalated chloride, nitrate, and carboxylate ions.[22,25−29] Although carbonate is ubiquitous among the II-III LDHs,[14] carbonate-containing Li−Al LDHs have not been fully explored.[24] In this paper we predict on the basis of the symmetry of the Li−Al layer the different possible polytypes of the carbonate-containing Li−Al LDHs, synthesize them, and in the process show that the Li−Al layer has all the features of a structural synthon.

EXPERIMENTAL SECTION

Synthesis. The Li−Al−CO_3 LDHs were prepared by various routes.

Coprecipitation. Li−Al−CO_3 LDHs were prepared by addition of a mixed metal (Li + Al) chloride solution ($[Li^+]/[Al^{3+}]$ = 0.5) to a solution containing five times the stoichiometric excess of Na_2CO_3. The reaction was carried out at a constant pH = 10 using a Metrohm model 718 Stat Titrino operating in STAT mode under constant stirring at room temperature.

Homogenous Precipitation by Hydrolysis of Urea. Solid urea was added to a mixed metal ($[Al^{3+} + Li^+]$ = 0.5 M) chloride solution while maintaining the molar ratio of [urea]/($[Al^{3+}] + [Li^+]$) at 3.3. The suspension was aged at 90 °C for 48 h.

Imbibition. Bayerite was prepared by ammonia precipitation following a literature procedure.[25] Gibbsite was provided by Jawaharlal Nehru

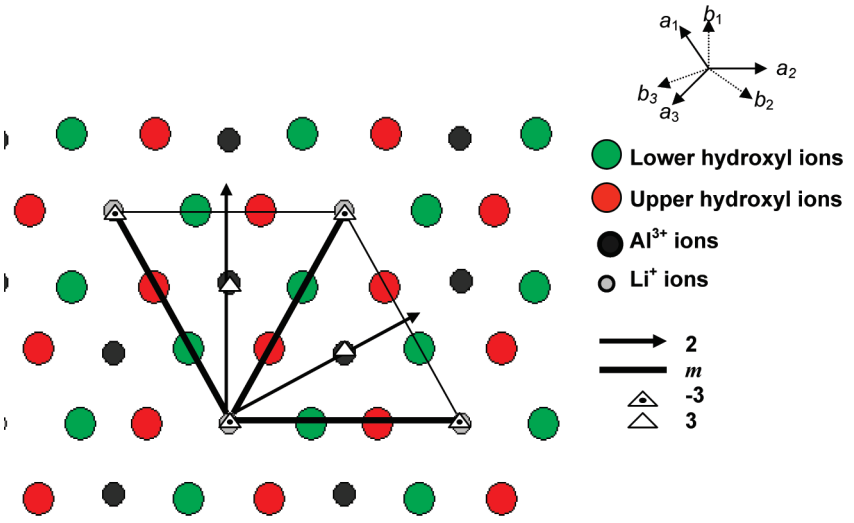

Figure 1. Li−Al layer viewed down the *c* axis. The principal symmetry elements are indicated.

Aluminum Research Development and Design Center (JNARDDC, Nagpur, India). The Li−Al−CO_3 LDHs were prepared by soaking 0.3 g batches of bayerite or gibbsite in ∼0.1 M Li_2CO_3 solution (volume 40 mL) followed by hydrothermal treatment in a Teflon-lined autoclave (50% filling) at 125−140 °C (24 h).

Anion Exchange. Li−Al−NO_3 LDHs were prepared by an imbibition procedure by soaking bayerite or gibbsite in ∼10 M $LiNO_3$ followed by hydrothermal treatment at 140 °C (24 h) as described above. An ∼0.25 g amount of the Li−Al−NO_3 LDH is stirred in 30 mL of a suspension containing 6 times molar excess of Na_2CO_3. The suspension is stirred at ambient temperature for 24 h.

All products were characterized by powder X-ray diffraction (Bruker D8 Advance diffractometer, Cu Kα radiation, λ = 1.5418 Å) operated in reflection geometry. Data were collected at a continuous scan rate of 1° min^{-1} and a step size of 0.02° 2θ. For Rietveld refinement, data were recorded over a 5−100° 2θ range (step size of 0.02° 2θ, counting time 10 s $step^{-1}$). Unit cell parameters were refined using the PROSZKI program.[30] Rietveld refinement was carried out using the GSAS software package.[31] For the refinement, a TCH pseudo-Voigt line shape function (Profile Function 2) with seven variables was used to fit the experimental profile. The background was corrected using a 6 coefficient Chebyschev polynomial. Anomalously, high intensities of basal reflections in the case of the gibbsite-derived LDH were corrected for by incorporating preferred orientation using the March−Dollase function wherein there is one refinable parameter, R_o, representing the crystal habit.

Wet chemical analysis of all single-phase preparations of the Li−Al−CO_3 LDHs was carried out. The Li content in the LDHs were estimated using flame photometry and Al content by gravimetric analysis. The intercalated water content was determined from thermogravimetry (TGA) data (Mettler Toledo TG/SDTA model 851^e system, 30−800 °C, heating rate 5 °C min^{-1}, flowing air). IR spectra were recorded using a Bruker Alpha-P IR spectrometer (ATR mode, 400−4000 cm^{-1}, 4 cm^{-1} resolution). Scanning electron micrographs were obtained using a JEOL model JSM 6490 LV microscope (operating voltage 15 kV). The powder samples were dispersed on a double-sided conducting carbon tape. The samples were sputter coated with Pt to improve conductivity.

Model simulations of the powder X-ray diffraction (PXRD) patterns were carried out using the program DIFFaX.[32] Within the DIFFaX formalism,[33] a solid is treated as a stacking of layers of atoms and the PXRD pattern computed by integrating the diffraction intensity layer by layer. This is ideally suited for layered materials where the layers exist naturally as a consequence of anisotropic bonding. For model simulations, the atomic coordinates of a single layer of the Li−Al−Cl LDH[22] with interlayer atoms excluded were used as input. The different polytypes were obtained by varying the stacking vectors, also called transitions, used to stack the layers one above the other. DIFFaX simulations of experimentally observed patterns were carried out using the metal hydroxide layer together with the interlayer atoms, as obtained from structures refined in this work.

RESULTS AND DISCUSSION

The Li−Al layered double hydroxides are most often prepared from gibbsite or bayerite by 'imbibition'[25] of a lithium salt, LiX, into $Al(OH)_3$ through a topochemical process. These layered solids may also be prepared by other routes such as coprecipitation, homogeneous precipitation, or anion exchange. The anisotropy in bonding that is characteristic of these materials implies that depending on the synthetic conditions and the nature of the anion, successive layers may be stacked one above the other in a number of ways to give a range of polytypes. In all such polytypes the constituent layers remain the same, and therefore, all possible polytypes may be derived using the same layer. The only structure refined to date in this system, aside from the refinement reported earlier by the authors of the present paper,[23] is the Li−Al−Cl LDH obtained from gibbsite.[22] The latter crystallizes in the $P6_3/m$ space group. A schematic of the single layer with the symmetry elements indicated is given in Figure 1. As in the precursor, the cations within the layer are ordered with the *a* parameter being characteristic of the distance between two Li ions. This layer constitutes a structural synthon. These layers are stacked one above the other to obtain the LDH crystal, and different stacking sequences yield different polytypes. It is our hypothesis that these layers stack in such a manner that conserves the symmetry elements of the single layer. In suggesting this hypothesis, we are guided by Verma and Krishna,[34] who correlate crystal symmetry with the enthalpy of formation by relating loss of symmetry with an overall reduction in the enthalpy of formation.

Symmetry of the Li−Al Layer. The symmetry of a single Li−Al layer corresponds to the layer group *P*-312/*m*. Two kinds of symmetry elements characterize this synthon: Symmetry

dx.doi.org/10.1021/ic200312g |*Inorg. Chem.* 2011, 50, 5619–5627

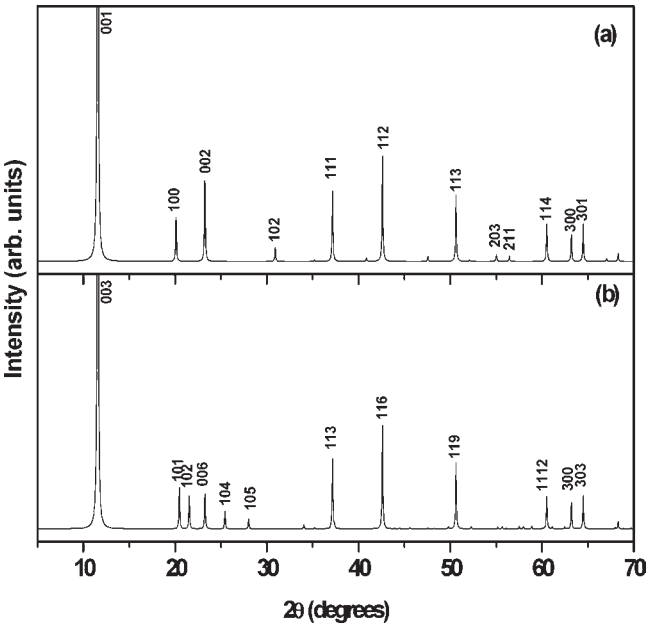

Figure 2. DIFFaX-simulated PXRD patterns of the (a) 1H and (b) 3R polytypes.

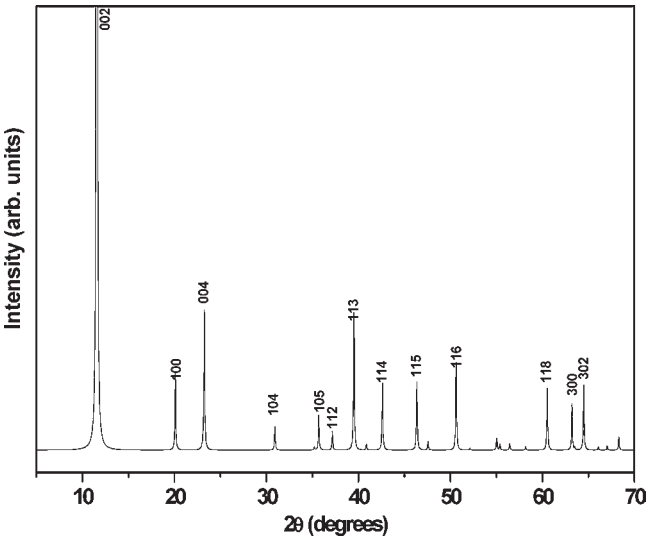

Figure 3. DIFFaX-simulated PXRD pattern of the 2H polytype.

elements that are perpendicular to the layer (the 3-fold axis and the mirror plane) and symmetry elements parallel with the layer (the 2-fold axis).

Stacking Sequences That Conserve the 3-Fold Axis. We first consider the polytypes that result on stacking successive layers in such a manner as to conserve the perpendicular symmetry elements. Three-fold axes perpendicular to the layer are present at (0, 0), (1/3, 2/3), and (2/3, 1/3) (Figure 1). Stacking one layer directly above the other, without any translation, results in a hexagonal polytype containing one layer in the unit cell. The DIFFaX-simulated PXRD pattern of this polytype, designated 1H, is given in Figure 2a. Translation of successive layers by (1/3, 2/3, z) results in a 3-layer polytype of rhombohedral symmetry (Figure 2b). We call this polytype 3R. A symmetrically equivalent orientation of adjacent layers arises on

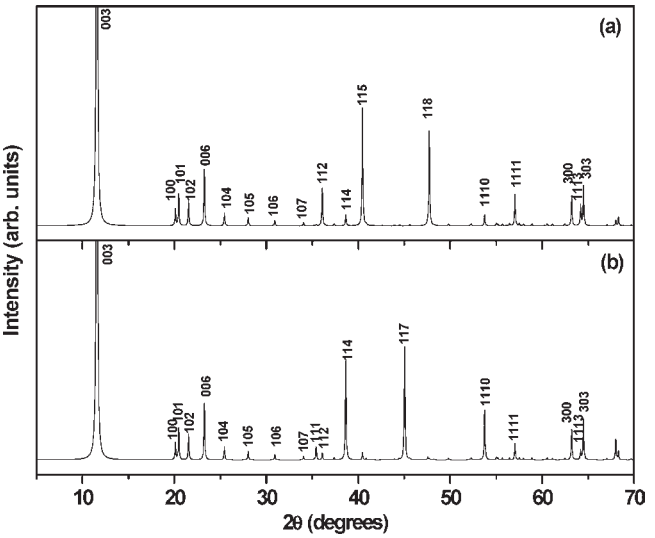

Figure 4. DIFFaX-simulated PXRD patterns of the (a) $1M_1$ and (b) $1M_2$ polytypes.

translation of successive layers by (2/3, 1/3, z) and gives rise to a PXRD pattern that is identical to that shown in Figure 2b. In all these stacking sequences the 3-fold symmetry of the single layer is conserved in going from one layer to the next. The PXRD patterns of the 1H and 3R polytypes differ only in the 10l series of reflections, which appear in the region between 20° and 30° 2θ and are indicative of the ordering of cations. The cations are ordered both within the layer (in the $a-b$ plane) as well as along the c direction.

Yet another way of stacking adjacent layers so as to conserve the 3-fold axis of the single layer is to reflect the single layer and stack the two layers alternatively one above the other, one being the mirror image of the other. In so doing, the 3-fold axis will become the subset of a 6_3 screw axis. As there are two layers per unit cell of hexagonal symmetry, we call this a 2H polytype (Figure 3). There is no other stacking that yields a symmetrically equivalent orientation of adjacent layers to this one.

Stacking Sequences That Conserve the 2/m Axis. We next consider the mirror plane perpendicular to the layer. Translation of successive layers along a_1 (or a_2) results in destroying the 3-fold axis perpendicular to the layer but retention of the mirror (which becomes a glide) and the 2-fold axis parallel to the layer.

For a start we consider translations of successive layers by (1/3, 0, z). As the upper and lower planes of hydroxyl ions within a single metal hydroxide layer are in an approximately hexagonal arrangement (approximate, on account of cation order within the layer), a translation of successive layers by (1/3, 0, z) results in the coincidence of the pseudo-3-fold axis of these two planes from one metal hydroxide layer to the next. From a symmetry retention point of view, such a translation is next best to the one described in the earlier section. It would also provide the most favorable packing of layers, compared to any other (random) translation along a_1. The PXRD pattern resulting from such a structure can be indexed to a 3-layered hexagonal (3H) cell. However, the most precise relationship between the nearest neighbors is best described by a 1-layered monoclinic cell, and therefore, we call this polytype $1M_1$. As the mirror along a_1 is symmetrically related to that along a_2 and a_3 by the 3-fold axis of the single layer, symmetrically equivalent orientations of adjacent

dx.doi.org/10.1021/ic200312g |*Inorg. Chem.* 2011, 50, 5619–5627

Table 1. Results of Wet Chemical Analysis and TGA Data[a]

sample	Li^+ (wt %)	Al^{3+} (wt %)	% mass loss from TGA (excluding adsorbed H_2O)	approximate composition of sample
Li−Al−CO_3 LDH (bayerite based)	2.6(2.4)	26.1(23.7)	49.5	$[Li_{0.26}Al_{0.66}(OH)_2][CO_3]_{0.13}\cdot 0.75H_2O$
Li−Al−CO_3 LDH (gibbsite based)	2.4(2.4)	25.5(24)	49.1	$[Li_{0.25}Al_{0.66}(OH)_2][CO_3]_{0.125}\cdot 0.72H_2O$

[a] Values in parentheses are expected from the approximate formula.

Table 2. Crystal Data and Structure Refinement Parameters of the Li−Al−CO_3 LDH Obtained from Gibbsite

cryst syst	hexagonal
space group	$P6_3/m$
cell params	$a = b = 5.0979(4)$ Å, $c = 15.1019(5)$ Å
vol./Å^3	339.902(5)
data points	4747
params refined	33
*R*wp	0.1763
*R*p	0.1068
$R(F^2)$	0.0989
*R*exp	0.0339

layers can be obtained by stacking successive layers with the vectors (0, 1/3, *z*) or (2/3, 2/3, *z*). All three stacking vectors give rise to PXRD patterns identical to that shown in Figure 4a.

A related polytype may be obtained by changing the translation component to (2/3, 0, *z*). The PXRD pattern characteristic of this polytype (Figure 4b) is identical to the pattern corresponding to translations of successive layers by (0, 2/3, *z*) or (1/3, 1/3, *z*). As this polytype is similar to the $1M_1$ polytype described above, differing only in the translational component, we call this polytype $1M_2$. The PXRD patterns of the $1M_1$ and $1M_2$ polytypes differ only in the regions between 30° and 70° 2θ. The two polytypes vary in the relative intensities of their 11*l* reflections. While $1M_1$ have prominent reflections for $l = 2$, 5, 8, and 11, $1M_2$ has prominent reflections for $l = 1$, 4, 7, and 10.

To summarize, the derived polytypes may be classified as follows:

1H (0, 0, *z*),
3R (1/3, 2/3, *z*) or (2/3, 1/3, *z*),
2H (0, 0, *z*) in which adjacent layers are mirror reflections of each other (mirror perpendicular to the stacking direction),
$1M_1$ (1/3, 0, *z*) or (0, 1/3, *z*) or (2/3, 2/3, *z*),
$1M_2$ (2/3, 0, *z*), or (0, 2/3, *z*) or (1/3, 1/3, *z*).

The polytypes derived here are by no means exhaustive, and in principle, an infinite number of possibilities arrived at by combinations of the above stacking vectors can be envisaged. However, our aim here is to describe the simplest polytypes, namely, those describable by a single stacking vector that best explains the methodology and reserve the consideration of more complex polytypes for future work.

Experimentally Obtained Polytypes. We ask the question, how many of these predicted structures can be experimentally realized? As an illustration, we consider the CO_3^{2-}-containing LDHs. Among layered materials such as these, polytype selection is often guided by the molecular symmetry of the anion.[18,35] Furthermore, reports on Li−Al LDHs containing carbonate are scarce.[22] Serna and co-workers[19] indexed the Li−Al−CO_3 LDH to a hexagonal cell. However, in later work, the carbonate-containing LDH was indexed to a monoclinic cell.[36] To resolve these ambiguities, we focus on the synthon approach to identify the structures of the Li−Al−CO_3 LDHs obtained by different routes.

We employ four different synthetic strategies for the preparation of these LDHs: (i) imbibition of Li_2CO_3 into the precursors gibbsite and bayerite, (ii) anion exchange of CO_3 for NO_3 using the Li−Al−NO_3 LDH derived from gibbsite (LAN-g) or bayerite (LAN-b) used as precursors, (iii) coprecipitation, and (iv) homogeneous precipitation by hydrolysis of urea.

Gibbsite-Based Li−Al−LDH. Imbibition of Li_2CO_3 into gibbsite does not yield a single-phase product. However, anion exchange of NO_3^- for CO_3^{2-} using LAN-g yielded a pattern (Supporting Information SI.1) which could be indexed to the 2H polytype described in the previous section. The IR spectrum of the anion-exchanged sample shows the extinction of the vibrations due to NO_3^- and the appearance of vibrations of intercalated carbonate (Supporting Information SI.2).

As the reflections of this pattern are sharp, indicating a high degree of crystallinity, we refine the structure of this anion-exchanged product using the structure of the gibbsite Li−Al−Cl LDH to provide a partial structure model. The atom positions of the Li−Al layer were obtained from this structure (CC 83512). The Al/Li ratio of 2.6 was obtained from chemical analysis (Table 1) and used in the refinement. We initially place the O2 oxygen (O atom of the intercalated H_2O/CO_3^{2-}) in a 6*h* position (0.351, 0.351, 0.25). Successive difference Fourier calculations yielded electron density (~1.4 e Å^{-3}) at one more 6*h* position (0.213, 0.213, 0.5) and a 2*d* position (0.666, 0.333, 0.25). The interlayer C was therefore placed at the 2*d* position and the water oxygen at the 6*h* position. A further cycle of refinement was carried out, and the difference Fourier map computed at this stage yielded no significant residual electron density (≲0.3 e Å^{-3}). The refinement details are given in Table 2, and the final refined atomic coordinates are given in Table 3. The C−O distance (1.33 Å) agrees with the C−O distance expected of carbonate (Table 4). In addition, the O1−O2 distances (2.76 Å) suggest hydrogen bonding between the oxygen of the hydroxyl groups of the layer and that of carbonate. The Rietveld fit of the PXRD pattern after the final cycle of refinement is shown in Figure 5.

Bayerite-Derived Li−Al LDH. We next look at the Li−Al LDHs obtained using bayerite as a precursor. The products obtained by imbibition, anion exchange, coprecipitation, and homogeneous precipitation yielded similar PXRD patterns, suggesting that they have the same structure (see Supporting Information SI.3). Intercalation of CO_3^{2-} is indicated by the IR spectrum which exhibits the antisymmetric stretching mode of CO_3^{2-} at 1365 cm^{-1} (Supporting Information SI.4). This phase could be indexed to both a 3-layered hexagonal cell as well as a 1-layer monoclinic cell (Table 5). Comparison with the simulated patterns in the previous section indicates that the structure corresponds to the $1M_1$ polytype. As the product obtained by imbibition of Li_2CO_3 into bayerite is the most crystalline, characterized by sharp and symmetric reflections, we attempt a refinement of this structure in the *C*2/*m* space group.[37] A Le Bail

dx.doi.org/10.1021/ic200312g |*Inorg. Chem.* 2011, 50, 5619–5627

Table 3. Refined Unit Cell and Atomic Parameters of the Gibbsite-Derived LDH after the Final Cycle of Refinement[a]

atom type	Wyckoff position	*x*	*y*	*z*	SOF	U_{iso}/Å^2
Li	2*b*	0.0	0.0	0.0	0.6	0.025
Al	4*f*	0.3333	0.6667	0.00669(29)	1.0	0.01279
O1	12*i*	0.6384(14)	0.6491(14)	0.56704(13)	1.0	0.025
O2	6*h*	0.4111(34)	0.343(6)	0.25	0.572	0.0423
O3	6*h*	0.214(7)	0.211(6)	0.25	0.523	0.1129
C	2*d*	0.6666	0.3333	0.25	0.305	0.8

[a] $a = b = 5.0979(4)$ Å, $c = 15.1019(5)$ Å.

Table 4. Selected Bond Distances (Å) of the Gibbsite-Derived Li−Al−CO_3 LDH

Li−O1	2.080(5)
Al−O1	1.917(7)
Al−O1	1.951(7)
C−O2	1.328(16)

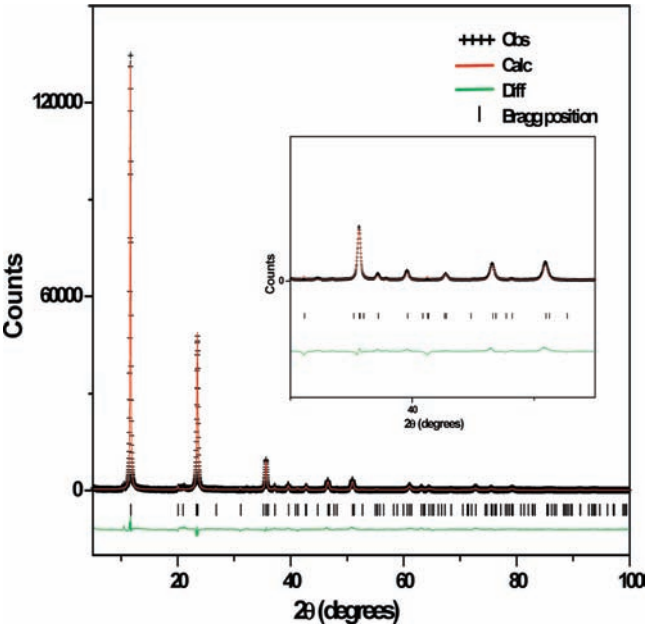

Figure 5. Rietveld fit of the observed PXRD profile of the gibbsite-derived Li−Al−CO_3 LDH. (Inset) Details of the fit in the 30−55° 2θ region.

fit was first carried out in this space group to determine accurate initial lattice parameters. After refinement of the cell parameters, background, scale, and profile parameters, a difference Fourier map was calculated to determine the interlayer atom positions which yielded residual electron density (~1.6 e Å^{-3}) in the interlayer at the 2*d* position (0, 0.5, 0.5). O3 was therefore placed at this position. Further cycles of refinement followed by calculation of the difference Fourier map yielded more residual electron density at the 4*h* (0.0, 0.384, 0.5), 4*h* (0.0, 0.155, 0.5), and 4*i* (0.190, 0.0, 0.5) positions. From the location of the maxima in the interlayer electron densities, the C atom was placed at the 4*i* position and O atom at the other positions. The Fourier map calculated after this stage was featureless. The details of the refinement are given in Table 6. The Rietveld fit of the

Table 5. Indexing of the Bayerite-Derived LDH

	monoclinic cell[a]		hexagonal cell[b]	
2θ(obs) (deg)	2θ(calcd) (deg)	*hkl*	2θ(calcd) (deg)	*hkl*
11.72	11.74	001	11.74	003
20.14	20.12	020	20.12	100
23.60	23.60	002	23.62	006
35.46	35.45	−130	35.45	111
35.74	35.73	003	35.76	009
36.12	36.13	−131	36.13	112
40.62	40.66	−132	40.66	115
48.08	48.09	−133	48.09	118
54.28	54.28	−204	54.24	11 10
57.64	57.65	−242	57.61	214
63.20	63.21	−331	63.21	300
64.50	64.53	061	64.53	303
68.46	68.44	062	68.48	306

[a] $a = 5.0954(2)$ Å, $b = 8.829(16)$ Å, $c = 7.725(2)$ Å, $\beta = 102.62(4)°$. [b] $a = b = 5.0965(8)$ Å, $c = 22.604(8)$ Å.

Table 6. Crystal Data and Structure Refinement Parameters of the Li−Al−CO_3 LDH Derived from Bayerite

cryst syst	monoclinic
space group	*C*2/*m*
cell params	$a = 5.087(9)$ Å, $b = 8.8200(17)$ Å, $c = 7.7016(6)$ Å, $\beta = 102.43(1)°$
vol./Å^3	337.49(4)
data points	4731
params refined	42
*R*wp	0.1976
*R*p	0.1432
$R(F^2)$	0.1291
*R*exp	0.0353

PXRD pattern after the final cycle of refinement is shown in Figure 6, and the refined atomic coordinates are given in Supporting Information SI.5. The calculated and observed profiles do not match in select regions (see, for instance, the 20−32° range of 2θ values). The observed peaks have a 'saw-tooth' line shape, while the calculated Bragg reflections have a symmetric line shape. The origin of these differences is more fully discussed below.

Disorder in the 1M$_1$ Polytype: Planar Faults versus Cation Disorder. We recall that while there is only one set of symmetry

dx.doi.org/10.1021/ic200312g |*Inorg. Chem.* 2011, 50, 5619–5627

operations giving rise to the 2H polytype, the 1M polytype is generated by two sets in both of which the same symmetry elements are conserved and which differ only in their translational components. While the $1M_1$ polytype may be generated by any of the following stacking vectors $(1/3, 0, z)$, $(0, 1/3, z)$, or $(2/3, 2/3, z)$, the $1M_2$ polytype may be generated by $(2/3, 0, z)$, $(0, 2/3, z)$, or $(1/3, 1/3, z)$. It would be expected that any orientation of adjacent layers which is symmetrically equivalent would also be energetically equivalent. It is therefore likely that in any polytype crystallizing in the $1M_1$ polytype (say, with the stacking vector $(1/3, 0, z)$), it is equally likely that the layers may be stacked with the other vectors belonging to the $1M_1$ polytype or with those of the $1M_2$ polytypes, giving rise to stacking faults.

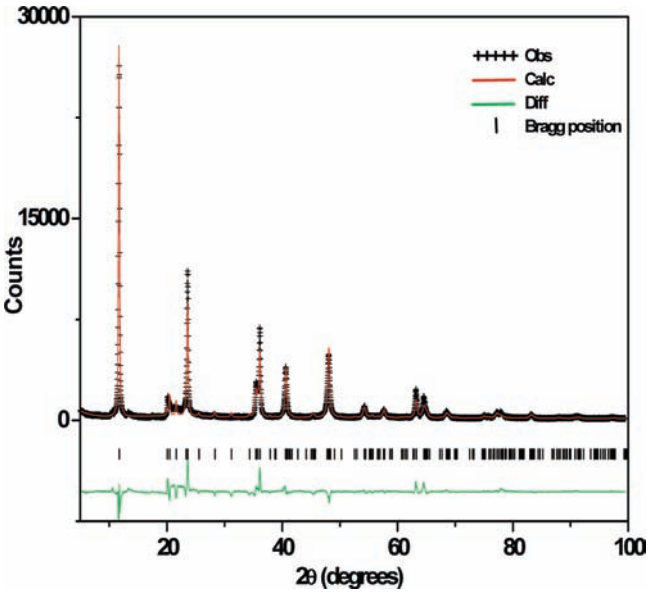

Figure 6. Rietveld fit of the observed PXRD profile of the bayerite-derived Li−Al−CO_3 LDH.

Each of the stacking vectors corresponding to the $1M_1$ polytype give rise to the same structure individually (Figure 4a). Combining two or more stacking vectors of the $1M_1$ polytype would retain all the symmetry elements of the $1M_1$ polytype and give equivalent orientations of hydroxyl groups across the interlayer region but destroy the ordering of cations along the *c* direction. The resulting structure would therefore be one with planar faults arising out of cation disorder along the *c* direction. A DIFFaX simulation of the $1M_1$ polytype using different percentages of the $(0, 1/3, z)$ and $(2/3, 2/3, z)$ stacking vectors (Figure 7a) results in the pattern acquiring an anisotropic broadening only in the region between 20° and 23° 2θ and extinction of the low-intensity reflections between 23° and 35° 2θ. These effects are often observed in patterns of Li−Al LDHs and are seen even when other reflections are symmetrically broadened (see Figure 6).

We next consider the $1M_1$ polytype with different percentages of planar faults corresponding to the $1M_2$ polytype. In this case, broadening of the mid-2θ reflections (30−60° 2θ) is observed at low % incidence of the stacking faults and broadening of all non-00*l* is observed at high % incidence of the stacking faults (Figure 7b).

The anisotropic broadening of lines observed in the experimental pattern is simulated in Figure 8. The good match is

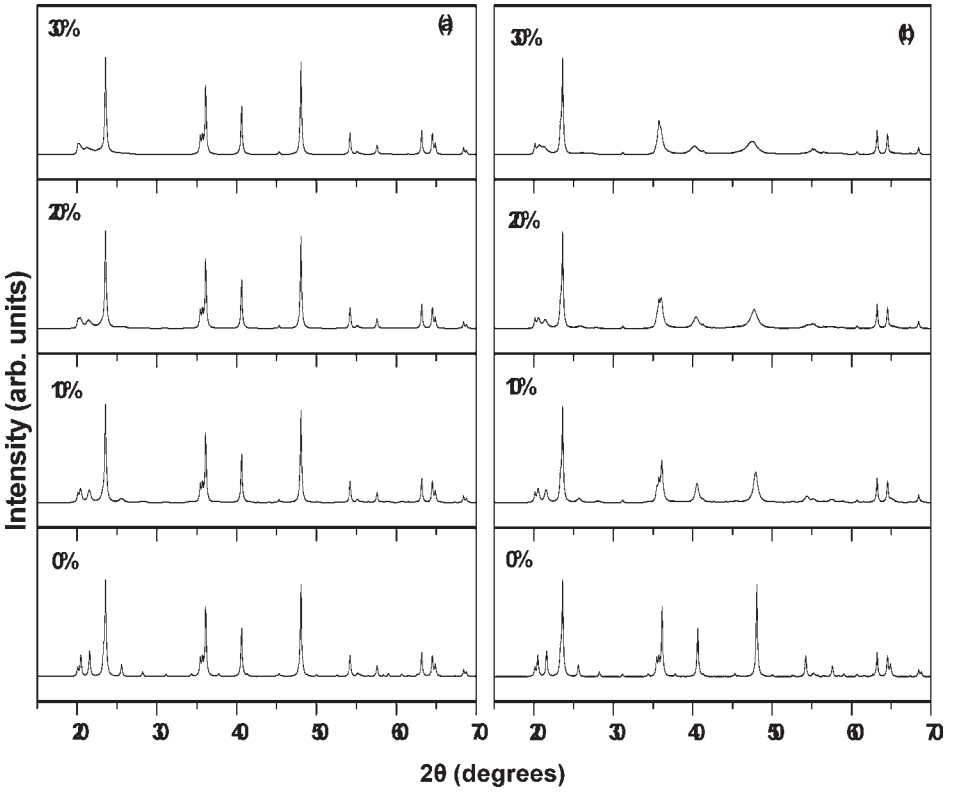

Figure 7. DIFFaX-simulated PXRD pattern of the $1M_1$ polytype (a) with cation disorder due to incorporation of different proportions of the symmetrically related stacking vectors of the $1M_1$ set and (b) with incorporation of different proportions of planar faults corresponding to the stacking motif of the $1M_2$ polytype. The 001 reflection is not shown for clarity.

dx.doi.org/10.1021/ic200312g |*Inorg. Chem.* 2011, 50, 5619–5627

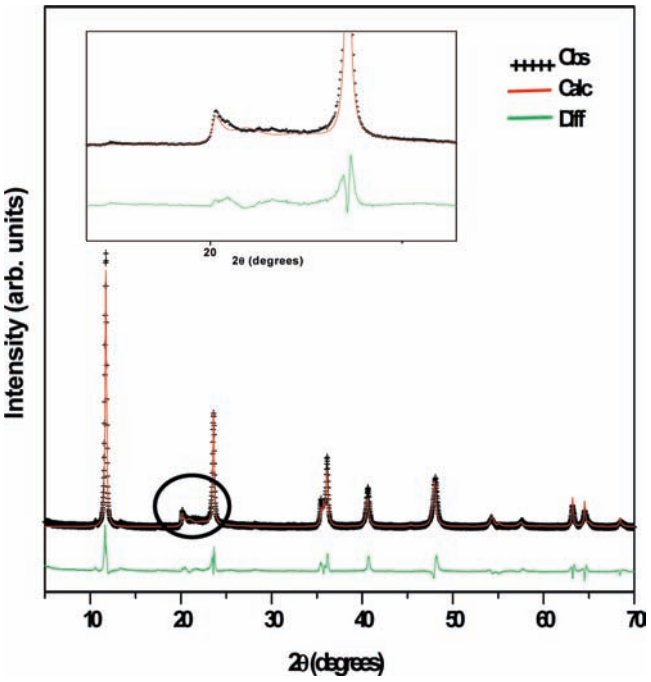

Figure 8. Comparison of the observed PXRD pattern of the Li−Al−CO_3 LDH obtained from bayerite with the DIFFaX-simulated pattern of the $1M_1$ constructed by a combination of symmetry-related stacking vectors and 6% of stacking faults of the $1M_2$ motif. Highlighted in the inset is the anisotropically broadened region.

obtained by combining equal proportions of the stacking vectors $(2/3, 2/3, z)$ and $(1/3, 0, z)$ corresponding to the $1M_1$ polytypes with 6% of stacking faults $(2/3, 0, z)$ of the $1M_2$ polytype. A visual inspection shows that this fit is superior to that obtained by Rietveld refinement shown in Figure 6. Further, the layer used for this simulation is obtained from the structure of the gibbsite-derived LDH, refined in Figure 5. That the same Li−Al−CO_3 layer yields the structure of both the bayerite- and gibbsite-derived LDHs shows that this layer is a structural synthon.

The morphologies of the gibbsite- and bayerite-derived carbonate LDHs, as exhibited by their SEM images (Figure 9), also reflects the underlying symmetry and topochemical mechanism of formation of these LDHs. The gibbsite-derived CO_3−LDH exhibits the same sharply faceted hexagonal morphology as the precursor gibbsite, while the bayerite-derived CO_3−LDH, like its precursor bayerite, exhibits no distinctive morphology.

It is seen that the stacking sequence of the Li−Al−CO_3 LDHs are strongly mediated by the symmetry of the CO_3 ion. Imbibition of Li_2CO_3 into bayerite is accompanied by a sliding of adjacent layers by $a/3$ resulting in the $1M_1$ polytype that offers approximate trigonal prismatic interlayer sites whose symmetry matches with that of CO_3^{2-}. Furthermore, as there is more than one stacking arrangement that leads to conservation of the same symmetry elements as the $1M_1$ polytype, this polytype often crystallizes with stacking faults while the 2H polytype (gibbsite derived) is a symmetrically unique stacking and therefore crystallizes without stacking faults and was amenable to a good refinement.

In conclusion, we show that a single layer of $[LiAl_2(OH)_6]^+$ (layer group $P\text{-}312/m$) acts as a building block for construction of a diverse class of polytypes belonging to the hexagonal and monoclinic crystal symmetries. These polytypes differ from one

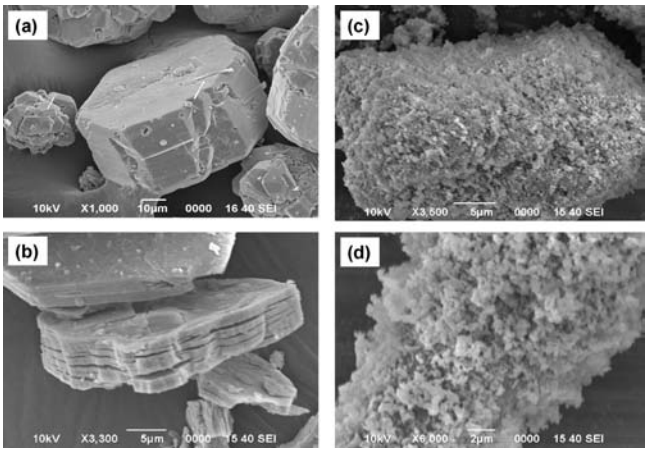

Figure 9. SEM images of (a) gibbsite, (b) the gibbsite-derived Li−Al−CO_3 LDH, (c) bayerite, and (d) the bayerite-derived Li−Al−CO_3 LDH.

another in the nature of anion packing as well as cation ordering along the stacking direction. However, the Li/Al layer is more than a building block, as it is not merely a topological entity but one that is derivable on the principles of crystal chemistry and layer group symmetry. These layers can be stacked in specific ways that either (i) conserve the principal symmetry elements of the layer group or (ii) systematically eliminate them to yield the universe of possible polytypes. By the use of appropriate precursors, we use topochemical pathways to synthesize a number of the predicted polytypes, refine their structures, identify the possible planar defects, and classify them according to their local symmetry.

Two other approaches closely compare with the structural synthon approach that we just outlined. (1) Implicit in Cario's approach[5,6] toward stacking 2D layers is conservation of the principal symmetry elements of the layer group. In as much as this approach does not provide a scope for the systematic elimination of the principal symmetry elements, it predicts only a subset of the possible structures that are predicted by the structural synthon approach. (2) An approach that closely resembles ours is provided by a theory of polytypism known as 'order−disorder theory' (OD theory),[38−40] which emphasizes the geometrical equivalence of adjacent layers in structures that exist as polytypes. This approach, though well cited in the mineralogical literature, has not been very popular in the wider community of crystal chemists, possibly due to its rigorous and pedagogical approach. The present treatment, although it has many parallels with 'OD theory', is an attempt to provide a much more simplified and intuitive approach to the prediction of polytypes of extended solids that is friendly to nonspecialists. The challenge remains however to extend the approach to other layered solids.

■ ASSOCIATED CONTENT

Supporting Information. PXRD data, IR spectra and refined atomic coordinates of the bayerite derived LDH. This material is available free of charge via the Internet at http://pubs.acs.org.

AUTHOR INFORMATION

Corresponding Author
*E-mail: vishnukamath8@hotmail.com.

ACKNOWLEDGMENT

The authors thank the Department of Science and Technology (DST), Government of India, for financial support. P.V.K. is a recipient of the Ramanna Fellowship of the DST. S.B. thanks the University Grants Commission for the award of a Senior Research Fellowship (NET).

REFERENCES

(1) Desiraju, G. R. *Angew. Chem., Int. Ed.* **1995**, *34*, 2311.
(2) Sarma, J. A. R. P.; Desiraju, G. R. *Cryst. Growth Design* **2002**, *2*, 93.
(3) Corey, E. J. *Pure Appl. Chem.* **1967**, *14*, 19.
(4) Jansen, M.; Schön, J. C. *Angew. Chem., Int. Ed.* **2006**, *45*, 3406.
(5) Cario, L.; Kabbour, H.; Meerschaut, A. *Chem. Mater.* **2005**, *17*, 234.
(6) Kabbour, H.; Cario, L.; Boucher, F. *J. Mater. Chem.* **2005**, *15*, 3525.
(7) Jansen, M.; Doll, K.; Schön, J. C. *Acta Crystallogr.* **2010**, *A66*, 518.
(8) Schön, J. C.; Jansen, M. *Int. J. Mater. Res.* **2009**, 135.
(9) Mellot-Draznieks, C.; Newsam, J. M.; Gorman, A, M.; Freeman, C. M.; Ferey, G. *Angew. Chem., Int. Ed.* **2000**, *39*, 2270.
(10) Mellot-Draznieks, C.; Girard, S.; Ferey, G.; Schon, J. C.; Cancarevic, Z.; Jansen, M. *Chem. Eur. J.* **2002**, *8*, 4102.
(11) Eddaoudi, M.; Moler, D. B.; Li, H.; Chen, B.; Reineke, T. M.; O' Keeffe, M.; Yaghi, O. M. *Acc. Chem. Res.* **2001**, *34*, 319.
(12) Murugavel, R.; Walawalkar, M. G.; Dan, M.; Roesky, H. W.; Rao, C. N. R. *Acc. Chem. Res.* **2004**, *37*, 763.
(13) Radha, S.; Antonyraj, C. A.; Kamath, P. V.; Kannan, S. *Z. Anorg. Allg. Chem.* **2010**, *636*, 2658.
(14) Cavani, F.; Trifiro, F.; Vaccari, A. *Catal. Today* **1991**, *11*, 173.
(15) Oswald, H. R.; Asper, R. *Preparation and crystal growth of materials with layered structures*; Lieth R. M. A., Ed.; D. Reidel Publishing Co.: Dordrecht, 1977; Vol. 1, p 71.
(16) Bookin, A. S.; Drits, V. A. *Clays Clay Miner* **1993**, *41*, 551.
(17) Bookin, A. S.; Drits, V. A. *Clays Clay Miner* **1993**, *41*, 558.
(18) Radha, A. V.; Shivakumara, C.; Kamath, P. V. *J. Phys. Chem. B.* **2007**, *111*, 3411.
(19) Serna, C. J.; Rendon, J. L.; Iglesias, J. E. *Clays Clay Miner* **1982**, *30*, 180.
(20) Megaw, H. D. *Z. Kristallogr.* **1934**, *87*, 185.
(21) Rothbauer, R.; Zigan, F.; O'Daniel, H. *Z. Kristallogr.* **1967**, *125*, 317.
(22) Besserguenev, A. V.; Fogg, A. M.; Francis, R. J.; Price., S. J.; O'Hare, D.; Isupov, V. P.; Tolochko, B. P. *Chem. Mater.* **1997**, *9*, 241.
(23) Britto, S.; Kamath, P. V. *Inorg. Chem.* **2009**, *48*, 11646.
(24) Britto, S.; Thomas, G. S.; Kamath, P. V.; Kannan, S. *J. Phys. Chem. C* **2008**, *112*, 9510.
(25) Poeppelmeier, K. R.; Hwu., S.-J. *Inorg. Chem.* **1987**, *26*, 3297.
(26) Fogg, A. M.; Freij, A. J.; Parkinson, G. M. *Chem. Mater.* **2002**, *14*, 232.
(27) Fogg, A. M.; Green, V. M.; Harvey, H. G.; O'Hare, D. *Adv. Mater.* **1999**, *11*, 1466.
(28) Fogg, A. M.; Dunn, J. S.; Shyu, S.-G.; Cary, D. R.; O'Hare, D. *Chem. Mater.* **1998**, *10*, 351.
(29) Lei, L.; Millange, F.; Walton, R. I.; O'Hare, D. *J. Mater. Chem.* **2000**, *10*, 1881.
(30) Lasocha, W.; Lewinski, K. *PROSZKI: A System of Programs for Powder Diffraction Data Analysis*, v. 2.4; Krakow, Poland, 1994. http://www.xray.cz/ecm-cd/soft/xray/index0098.html.
(31) Larson, A. C.; Von Dreele, R. B. *General Structure Analysis System (GSAS)*; Los Alamos National Laboratory Report LAUR 86-748, 2004.
(32) Treacy, M. M. J.; Deem, M. W.; Newsam, J. M. *Computer Code DIFFaX*, Version 1.807; NEC Research Institute, Inc.: Princeton, NJ, 2000.
(33) Treacy, M. M. J.; Newsam, J. M.; Deem., M. W. *Proc. R. Soc. London* **1991**, *A433*, 499.
(34) Verma, A. R.; Krishna, P. *Polymorphism and Polytypism in Crystals*; John Wiley: New York, 1966; p 33−60.
(35) Radha, S.; Kamath, P. V. *Cryst. Growth Design* **2009**, *9*, 3197.
(36) Sissoko, I.; Iyagba, R.; Sahai, R.; Biloen, P. *J. Solid State Chem.* **1985**, *60*, 283.
(37) Thiel, J. P.; Chiang, C. K.; Poeppelmeier., K. R. *Chem. Mater.* **1993**, *5*, 297.
(38) Dornberger-Schiff, K. *Acta Crystallogr.* **1956**, *9*, 593.
(39) Dornberger-Schiff, K.; Grell-Niemann, H. *Acta Crystallogr.* **1961**, *14*, 167.
(40) Dornberger-Schiff, K. *Acta Crystallogr.* **1982**, *A38*, 483.